Proceedings of the 3rd International Conference on Green Energy, Environment and Sustainable Development (GEESD2022), X. Zhang et al. (Eds.)

doi:10.3233/ATDE220265

Analysis of Grid-Connected Wind Turbine Generators on Power System Stability

Pengfei LI[1], Zeyuan LIN, Zhiyong ZHOU and Yanli LI
Shandong Electric Power Engineering Consulting Institute Corp., Ltd., Jinan, Shandong, China

Abstract. With the gradual integration of large wind farms, the wind power penetration in power system is gradually increasing. Since different wind turbines access grid may have different effects on the system, it is necessary to study the effect of different wind turbines access grid on the system transient stability. This paper makes a comparative study on the system stability of constant speed wind turbine (CSWT) and the doubly-fed induction generator (DFIG) after grid-connected. Firstly, we present the dynamic models of CSWT and DFIG. Then, we use IEEE 3-machine 9-bus system to study the effect of CSWT and DFIG connected to the system on the system transient stability under different wind power penetration. Simulation results show that with the increase of wind power penetration, the transient stability of the system shows a trend of increasing first and then decreasing. However, DFIG will deteriorate the system transient stability as wind power penetration increases.

Keywords. Power system, wind power penetration, DFIG, CSWT, transient stability

1. Introduction

Wind energy technology has been greatly developed in recent years. China's wind power cumulative installed capacity was 32.848 million kW, up 16.6% year-on-year, accounting for 13.9% of the country's installed power generation capacity [1]. New energy new installed capacity and total installed capacity ranked first in the world for many years [2]. Under the guidance of China's "carbon peak, carbon neutralization" goal, wind power penetration is increasing year by year [3]. In order to ensure the stable operation of the power system, it is essential to study the effect of different wind turbines on the transient stability of the system as the penetration rate increases [4, 5].

The impact of wind farm on system stability has been concerned. References [6-8] analyzed the influence of DFIG on the low-frequency oscillation characteristics and damping characteristics of the system after grid-connected; Reference [9] analyzed the influence of CSWT on the transient stability of the system at different wind power penetration rate wind power penetrations; Reference [10] compared and analyzed the influence of different capacity DFIG at the same node and different nodes the system transient stability ; Reference [11] compared the effects of different wind turbines on transient stability and small signal stability of the system under the same wind power

[1] Corresponding Author, Pengfei LI, Shandong Electric Power Engineering Consulting Institute Corp., Ltd., Jinan, Shandong, China; Email: 303510897@qq.com.

penetration; Reference [12] analyzed the changes of wind turbine rotor angle, bus voltage and reactive power after the grid connection of different types of wind turbines, but it did not involve the study of transient stability and low-frequency oscillation characteristics of the system.

This paper focuses on the influence of CSWT and DFIG on the system transient stability when connected to systems with different magnetic permeability. Moreover, his paper analyzes the dynamic model of CSWT and DFIG; using IEEE 3-machine 9-bus system as the test system, the effect of different turbine permeability on power system stability is comprehensively simulated and analyzed, and some preliminary meaningful conclusions are obtained.

2. Wind Turbine Dynamic Model and Stability Analysis

2.1. Constant Speed Wind Turbine

The CSWT consisting of blades, gears, constant speed asynchronous generators and parallel capacitors is connected to the grid through a boost transformer, as shown in Figure 1.

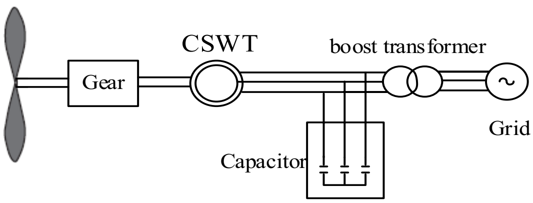

Figure 1. Dynamic model of CSWT.

The model uses a six-order model, and the six state variables are wind speed: v_w; wind turbine speed: w_t; generator rotor angular velocity: w_m; inter-axis twist angle λ; transient electromotive force of d-axis and q-axis: $e_d^{'}$, $e_q^{'}$.

$$\begin{cases} P_w = \dfrac{\rho}{2} C_p A_r v_w^3 \\ \dfrac{dw_t}{dt} = \dfrac{T_t - K_s \gamma}{2H_t} \\ \dfrac{dw_m}{dt} = \dfrac{K_s \gamma - T_e}{2H_m} \\ \dfrac{d\gamma}{dt} = 2\pi f (w_t - w_m) \\ \dfrac{de_d^{'}}{dt} = 2\pi f (1 - w_m) e_q^{'} - \dfrac{[e_d^{'} - (x_s + x_\mu - x^{'}) i_q]}{(x_r + x_\mu)/(2\pi f r_r)} \\ \dfrac{de_q^{'}}{dt} = -2\pi f (1 - w_m) e_d^{'} - \dfrac{[e_q^{'} + (x_s + x_\mu - x^{'}) i_d]}{(x_r + x_\mu)/(2\pi f r_r)} \\ x^{'} = x_s + \dfrac{x_r x_\mu}{x_\mu + x_r} \end{cases} \tag{1}$$

In the equation, ρ is the air density; C_P denotes the wind energy utilization factor [13]; A_r denotes the swept area of the wind turbine blade; f denotes the rated frequency of the grid; T_t denotes Wind turbine output mechanical torque; T_e denotes the electrical torque of the generator; H_t denotes the wind turbine inertia time constant; H_m denotes the inertia time constant of the generator; K_s denotes the inter-axis stiffness coefficient; i_d denotes d-axis current; i_q denotes q-axis current; r_r denotes rotor resistance; x_r denotes rotor reactance; x_s denotes stator reactance; x_μ denotes excitation reactance.

The tower shadow effect is taken into account in the establishment of the model. On the basis of the output torque of the wind turbine, a small amplitude periodic torque fluctuation is added; The transmission adopts a two-mass-spring model, which converts its inertia and stiffness to the high speed shaft side; The simplified electric circuit of CSWT is similar to the model of single squirrel cage induction motor, so the model can be established by d-axis, q-axis and reference angle of circuit network.

2.2. Doubly-Fed Induction Generator

Typical structures of DFIG are shown in Figure 2. DFIG consists of blades, gears, doubly fed generators and inverters. It is connected to the grid through a boost transformer. Its stator winding is connected to the grid directly, and the rotor winding is connected through a partial capacity converter.

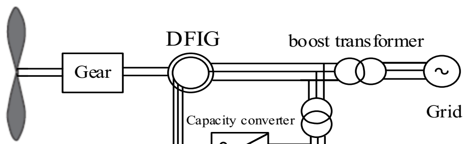

Figure 2. Dynamic model of DFIG.

The model uses a six-order model, and the six state variables are wind speed: v_w; generator rotor angular velocity: w_m; pitch angle: θ_p, d-axis and q-axis current: i_{dr}, i_{qr}.

$$\begin{cases} P_w = \dfrac{\rho}{2} C_p(\lambda, \theta_p) A_r v_w^3 \\ \dfrac{dw_m}{dt} = \dfrac{T_t - T_e}{2H_m} \\ \dfrac{d\theta_p}{dt} = \dfrac{[K_p \varphi(\omega_m - \omega_{ref}) - \theta_p]}{T_p} \end{cases} \qquad \begin{cases} \dfrac{di_{qr}}{dt} = [-\dfrac{x_s + x_\mu}{x_\mu V} p_w^*(\omega_m) / \omega_m - i_{qr}] \dfrac{1}{T_\xi} \\ \dfrac{di_{dr}}{dt} = K_v(V - V_{ref}) - v_h / x_\mu - i_{dr} \end{cases} \tag{2}$$

In the equation, λ is tip speed ratio ; C_P is the wind energy utilization factor [13]; K_P

is pitch angle control gain; T_P is pitch angle control time constant; ω_{ref} is the reference speed; $\varphi(\omega_m - \omega_{ref})$ is linear function of rotational speed ω_m . V_{ref} is the reference voltage calculated by the initial step; K_v is voltage control gain; T_ξ is power control time constant; $p_w^*(\omega_m)$ is the function of output power and speed of a wind turbine.

DFIG increases pitch angle control model and inverter model compared with CSWT. The transmission device adopts the single mass-spring model, that is, it is assumed that the control of the inverter can filter out the dynamic response between the generator rotor shaft and the high-speed shaft, thus the tower shadow effect is not considered. The mathematical model of DFIG is similar to that of single squirrel-cage induction motor, and the only difference is that the rotor winding has no short circuit, so the rotor voltage is not equal to zero. The inverter is regarded as an ideal current source, which simplifies the dynamic model of the inverter, because the inverter has faster response speed than the electromechanical transient process.

Due to the limited space, only the dynamic model of the fan is briefly summarized. The detailed mathematical model is found in the literature.

2.3. Transient Stability

At present, there are two common methods to analyze power system transient stability: forward Euler method and implicit trapezoidal method. Both methods leverage a Jacobi matrix to predict the direction of algebra and state variables at each step.

At time t, given a time step of Δt, the differential algebraic equations of the system can be expressed as:

$$\begin{cases} 0 = f_n[x(t+\Delta t), y(t+\Delta t), f(t)] \\ 0 = g[x(t+\Delta t), y(t+\Delta t)] \end{cases} \tag{3}$$

In this equation, f is the differential equation; g is an algebraic equation; f_n depending on the numerical integration method used. Implicit trapezoidal method is used in this paper.

Initial Values of System Operating State Equations before Disturbance Based on Power Flow Calculation Program. Alternate solutions of differential equations representing state variables and algebraic equations representing network structure in equation (3). The state variables and algebraic variables of the whole system at each time are obtained by implicit trapezoidal method. The stability of the system is judged by the relative swing angle of the synchronous motor, the speed and the curve of the voltage of each node with time.

3. Stability Analysis

This paper uses the IEEE 3-machine 9-bus system shown in Figure 3 as an example for the study, The relevant parameters of the system can be found in the reference, system benchmark capacity is 100 MVA, frequency is 60 Hz. Three synchronous generators use a two-axis model. The excitation mode is IEEE type I excitation. Generator G1 set to balance unit. Modeling of wind farm with single isoline, capacity 100*2MW, and the bus 7 is connected to the 230 kV line after boosting through two transformers, transformer and line parameters see reference [9]. Wind turbine models are considered for CSWT and DFIG. See Appendix for Parameters of Various Wind Turbines. Wind speed sample curves are simulated using the Weibull model, the follow-up analysis is based on this wind speed sample. Simulation completed by PSAT [14] software.

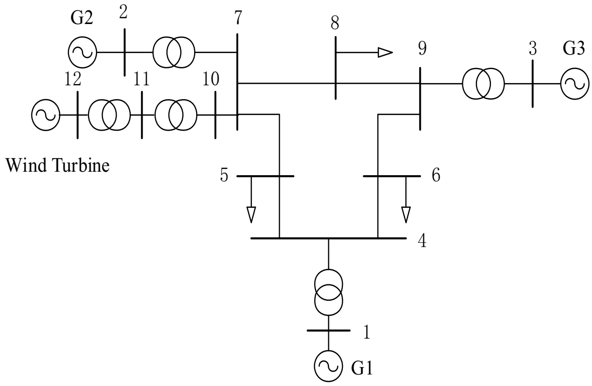

Figure 3. Modified three-machine nine-bus system.

3.1. Influence of Different Wind Turbine Generators on System Transient Stability

When $t = 1s$, a three-phase short-circuit fault occurs in the line between bus 5 and bus 7 in the vicinity of bus 7 (bus 7 fault has the greatest impact on system stability [14]), and the fault clearance time is $1.167s$. The line is re-entered at $t = 1.2s$ after the fault is cleared and the simulation time is 20s. To study the effect of wind power penetration from 0% to 60% with a step spacing of 10% on the system transient stability after different wind turbines are connected. Due to the limitation of space, four typical cases with penetration rates of 20% and 40% are selected for detailed analysis: (a) CSWT access system at 20% wind power penetration rate. (b) CSWT access system at 40% wind power penetration. (c) DFIG access system at 20% wind power penetration. (d) DFIG access system at 40% wind power penetration. Figure 4 shows the relative work angle, speed and node voltage versus time curves of the generator after a three-phase short-circuit fault in the system in four cases. In the figure $\delta_{Syn\,21}$ is the power angle of generator 2 relative to generator 1. $\omega_{Syn\,1}$, $\omega_{Syn\,2}$, $\omega_{Syn\,3}$ are the speeds of synchronous generators 1, 2 and 3 respectively and $V_{Bus\,01}$, $V_{Bus\,02}$, $V_{Bus\,03}$, $V_{Bus\,12}$ are the voltages at nodes 1, 2, 3, and 12, respectively.

The following conclusions can be drawn from Figure 4:

(1) Compared with the curves in Figures 4a and 4b, it can be seen that when the CSWT is connected to the system, after a fault occurs the first swing angle of the relative work angle of the generator at 20% penetration rate is 0.55 *rad* (31.5°); the first swing angle is 0.35 *rad* (20.1°) at 40% penetration rate. As the wind power penetration increases, the first swing angle of the synchronous generator relative power angle decreases.

At 20% penetration, after the fault occurred the relative work angle, speed and voltage at each node of the generator stabilized after 15s; At 40% penetration, after the fault occurred the relative work angle, speed and voltage at each node of the generator stabilized after 10s.

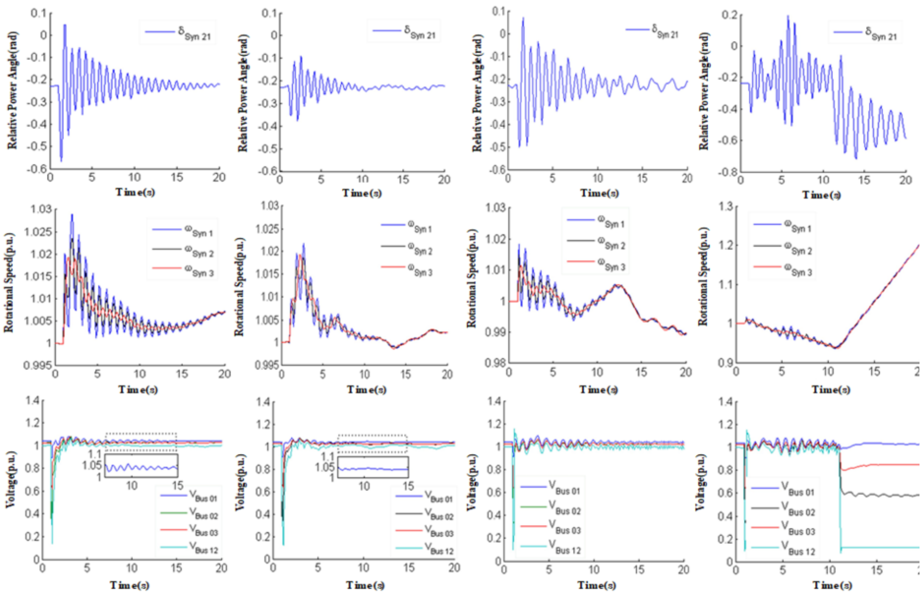

(a) 20% penetration level (CSWT)
(b) 40% penetration level (CSWT)
(c) 20% penetration level (DFIG)
(d) 40% penetration level (DFIG)

Figure 4. Fault response curves of four cases.

In the process of increasing the wind power penetration from 0% to 40%, the relative work angle, speed and node voltage curve fluctuations of the generator become smaller, and the system reaches stability faster, improving the system transient stability.

However, when the wind power penetration of constant speed wind turbine increases from 40% to 60%, the first swing angle of synchronous generator relative work angle increases, the generator relative work angle, speed and node voltage curve fluctuations become larger, the time to reach stability becomes longer, and finally the synchronous motor stalls, the node voltage drops suddenly, and the system is destabilized. Figure 5 shows the fault response curve for a CSWT connected to the system at a 60% penetration rate.

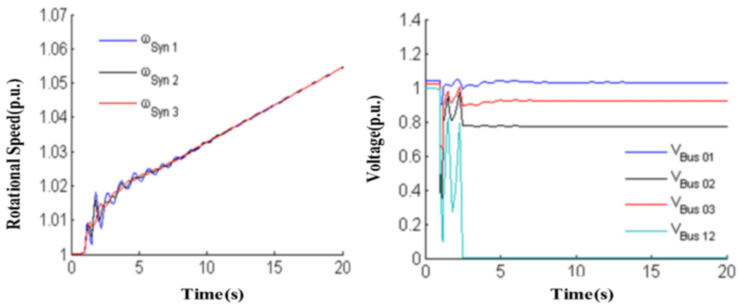

Figure 5. Fault response curves at 60% penetration level (CSWT).

(2) Comparing the curves in Figures 4a and 4c, it can be seen that at 20% penetration rate both CSWT connected to the system and DFIG connected to the system are

stabilized after the occurrence and removal of a three-phase fault, but after the fault occurs the latter has larger fluctuations in the relative power angle and slight fluctuations in the voltage at each node until the end of the simulation time. Moreover, the terminal voltage (node 12) of the latter wind turbines showed two tip pulses (overshoot and undershoot phenomenon) at the time of failure. Such voltage fluctuations may cause damage to the equipment and reduce its service life.

(3) Comparing the curves in Figures 4b and 4d, it can be seen that when the CSWT access system, after a fault occurs the system stabilizes after a slight oscillation at 40% penetration rate. However, when DFIG are connected, the system tends to stabilize after a fault occurs at 0% to 30% penetration, and at 40% penetration the system becomes unstable at about 11s after a fault occurs when the synchronous motor is out of step, the voltage at each node drops suddenly, and the system becomes unstable.

4. Conclusion

With the 3-machine 9-bus system, we analyze the influence on transient stability of the power system at different wind power penetration after CSWT and DFIG are connected respectively, and draw the conclusion: In the event of a three-phase short-circuit fault in the system, as the wind power penetration increases, the access of CSWT causes the transient stability of the system to show a trend of first increasing and then decreasing, and there exists an optimal wind power penetration access ratio; while the access of DFIG deteriorates the transient stability of the system.

Acknowledgments

This paper is supported by the project "Shandong Electric Power Engineering Consulting Institute Science and technology project" (37-2021-34-K0008).

References

[1] National Energy Administration. National Energy Administration Releases National Power Industry Statistics for 2021. http://www.nea.gov.cn/2022-01/26/c_1310441589.html, 2022-01-26/2022-03-06.

[2] National Energy Administration. Letter Concerning Reply to Proposal 1546 (Telecommunications 249) of the Fourth Session of the Thirteenth National Committee of CPPCC. 2022. http://zfxxgk.nea.gov.cn/2022-03/04/c_1310498429.html

[3] Zhao XL, Gong M, Fu B, Ma JM. An AGC method considering the variation of wind power permeability. Power Grid and Clean Energy. 2020;36(01):84-90.

[4] Xue AC, Fu XY, Qiao DK, Wang YJ, Wang JW. Review and prospect of sub-synchronous oscillation mechanism of power system involving wind power. Electric Power Automation Equipment. 2020;40(09):118-28.

[5] Wang YJ, Du WJ, Wang HF. Review on small signal stability of large-scale wind power gathering system. Power Grid Technology. 2022;1-13.

[6] Mou PT, Zhao DM, Wang JC. Mechanism analysis of influence of large-scale wind power access on system power angle stability. Proceedings of the CSEE; 2017;37(05):1325-34.

[7] Qi J, Wu Q, Chen K, Zhou D, Weng GQ. Additional Damping control for large-scale doubly-fed wind power generation system with time-varying delay. Power Grid Technology. 2019;43(12):4440-50.

[8] Zhou JC, Peng XT, Luo P, Liang K, Zhang Z. Damping characteristics of sub-synchronous control interaction of doubly-fed fan based on compound torque coefficient method. The Grid Technology. 2020;44(04):1247-57.

[9] EI SM, Badr MAL, Rassem OM. Impact of large scale wind power on power system stability. 12th International Middle East Power System Conference; Aswan, Egypt: South Valley University; 2008. p. 630-6.
[10] Zhang XJ, Sun SY, Zheng XY, Zhao W, Wang CY. Transient stability analysis of infinite single-machine system with wind power expansion under asymmetrical failure. Modern Power. 2020;37(04):368-75.
[11] He P, Wen FS, Xue YS, et al. Impacts of different wind power generators on power system small signal and transient stability. Automation of Electric Power Systems. 2013;37(17):23-9.
[12] Mrehel OG, Shenbisha A, Abdurasoul AS. Comparative study on effect of different wind generator types on power systems stability. 2021 IEEE 1st International Maghreb Meeting of the Conference on Sciences and Techniques of Automatic Control and Computer Engineering MI-STA; IEEE; 2021; p. 412-7.
[13] J G Slootweg. Wind Power: Modelling and Impact on Power System Dynamics. Delft University of Technology, Delft, Netherlands, 2003.
[14] Milano F. An open source power system analysis toolbox. IEEE Transactions on Power Systems. 2005, 20(3): 1199-1206.